PHYSICAL REVIEW FLUIDS **2**, 052601(R) (2017)

Shock-driven transition to turbulence: Emergence of power-law scaling

D. Olmstead,[1] P. Wayne,[1] D. Simons,[1] I. Trueba Monje,[1] J. H. Yoo,[1] S. Kumar,[2]
C. R. Truman,[1] and P. Vorobieff[1]

[1]*Department of Mechanical Engineering, University of New Mexico, Albuquerque, New Mexico 87131, USA*
[2]*Indian Institute of Technology Kanpur, Kanpur, Uttar Pradesh 208016, India*

(Received 30 December 2016; published 25 May 2017)

We consider two cases of interaction between a planar shock and a cylindrical density interface. In the first case (planar normal shock), the axis of the gas cylinder is parallel to the shock front and baroclinic vorticity deposited by the shock is predominantly two dimensional (directed along the axis of the cylinder). In the second case, the cylinder is tilted, resulting in an oblique shock interaction and a fully-three-dimensional shock-induced vorticity field. The statistical properties of the flow for both cases are analyzed based on images from two orthogonal visualization planes, using structure functions of the intensity maps of fluorescent tracer premixed with heavy gas. At later times, these structure functions exhibit power-law-like behavior over a considerable range of scales. Manifestation of this behavior is remarkably consistent in terms of dimensionless time τ defined based on Richtmyer's linear theory within the range of Mach numbers from 1.1 to 2.0 and the range of gas cylinder tilt angles with respect to the plane of the shock front (0–30°).

DOI: 10.1103/PhysRevFluids.2.052601

Richtmyer-Meshkov instability (RMI) [1,2] develops on an impulsively accelerated density interface, often manifesting in shock-accelerated gases with density gradients. Richtmyer-Meshkov instability is responsible for vortex formation in a number of problems, from astrophysical [3] and geophysical [4] to engineering applications such as inertial confinement fusion [5] and supersonic combustion [6]. In laboratory experiments and modeling, RMI-driven transition to turbulence also possesses features that make it an attractive test case for the more general problem of turbulent transition, namely, well-characterized and highly repeatable initial conditions combined with a finite and clearly defined energy input driving the flow.

The growth of RMI is usually described in a sequence of stages [7,8]. During the initial (linear) stage, the growth is to some extent consistent with Richtmyer's original theory [1] and is well described with compressible linear theory [9]. As initial vorticity deposition due to the misalignment of pressure and density gradients leads to roll-up of vortices, the second stage of nonlinear vorticity-dominated deterministic growth follows [10,11]. At the same time, secondary instabilities due to shear and secondary baroclinic effects emerge, leading to the next stage, where deterministic and disordered flow features coexist, and eventually to turbulence.

Consider an interfacial perturbation with a wavelength λ (with the corresponding wave number $\kappa = 2\pi/\lambda$) and amplitude a_0. Let the interface initially separate gases of densities ρ_1 and ρ_2 and be accelerated with a shock of Mach number M. The perturbation growth will depend in a nontrivial way on M, the Atwood number $A = (\rho_2 - \rho_1)/(\rho_2 + \rho_1)$, initial interfacial geometry, the extent of diffusion at the interface, etc. In the simplest case (Richtmyer's linear theory for a sharp periodically perturbed interface), the perturbation growth rate can be described as

$$|v^{\mathrm{imp}}| = \kappa a_0 A \Delta V, \tag{1}$$

where ΔV is the piston velocity of the shocked flow, dependent on the Mach number. Unlike the related Rayleigh-Taylor instability, which is gravity driven and thus has a constant supply of energy, the energy provided to produce the growth of RMI is finite and thus the growth generally slows with time. Several models exist to describe the RMI growth rate, from well-considered theories [11] to semiempirical equations [12].

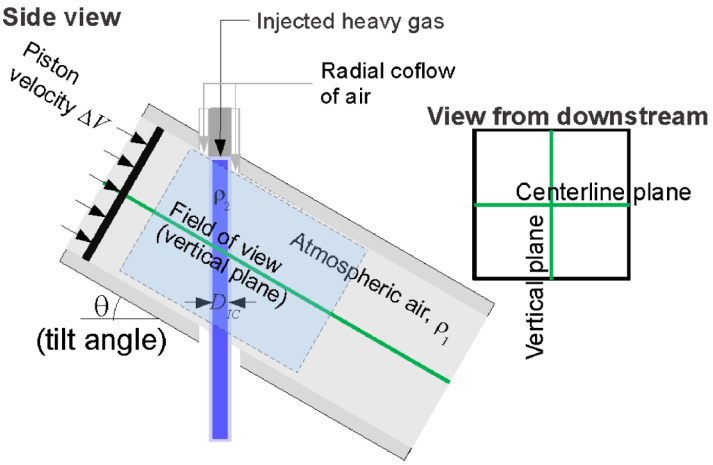

FIG. 1. Experimental setup: side view and view from downstream showing the centerline and vertical visualization planes.

During the subsequent stage of evolution, the RMI-driven mixing flow is known to develop features consistent with transition to turbulence: greatly enhanced mixing (mixing transition [12]) and power-law scalings of structure functions of scalar tracer advected by the flow [13] and of velocity [14] consistent with classical predictions for fully developed turbulence [15–17]. Until recently, experimental studies of RMI-driven transition to turbulence were largely confined to a situation when the initial conditions are nominally two dimensional, leading to formation of large-scale vortices with vorticity initially confined to one direction. Here we present a comparative study of shock-driven transition to turbulence evolving from such nominally two-dimensional conditions and from conditions when initial vorticity deposition is inherently three dimensional and find that the scalings of emerging turbulence are remarkably consistent for the geometries we investigate.

The experiments described here were conducted at the University of New Mexico (UNM) shock tube [18,19] (Fig. 1). Gravity-driven flow through a cylindrical nozzle produced the initial conditions, with a diffuse interface forming between a heavy gas (mixture of 89% SF_6 and 11% of acetone tracer by volume) injected through the nozzle into a test section of the shock tube, the latter being filled with quiescent air at ambient pressure. The measured Atwood number characterizing this diffuse interface is 0.6. Planar laser-induced fluorescence (PLIF) is induced in acetone tracer by illuminating a planar section of the flow with a pulsed UV laser sheet at a wavelength 266 nm. A distinctive feature of the UNM shock tube is that it can be tilted with respect to the horizontal by an angle θ, making it possible to create initial conditions both for planar normal (quasi-two-dimensional) and oblique shock interaction with density interfaces.

In the experiments presented here, the initial geometry of the density interface was cylindrical, with the axis of the heavy-gas cylinder inclined at an angle θ with respect to the plane of the shock. This density interface was produced by vertical injection of SF_6 with acetone tracer into the test section of the shock tube through a cylindrical nozzle (diameter $D_{IC} = 6.35$ mm). The gravity-driven heavy gas flow was stabilized by concentric coflow of air, resulting in a highly repeatable laminar diffuse interface. As the flow of the heavy gas was always directed straight down, to produce a desired angle θ, the shock tube itself was inclined at angles $\theta = 0$, 20°, and 30° with the horizontal (Fig. 1). The evolution of the flow was visualized in two planes. The first (vertical) plane is also labeled as the field of view in Fig. 1. The second (centerline) plane is oriented at 90° to the vertical plane, parallel to the flow direction, and is equidistant from the upper and lower boundaries of the test section of the shock tube. Thus we refer to it as the centerline plane. At $\theta = 0$ the centerline plane would be horizontal; at other angles, it is inclined with the shock tube. Images in the visualization planes were

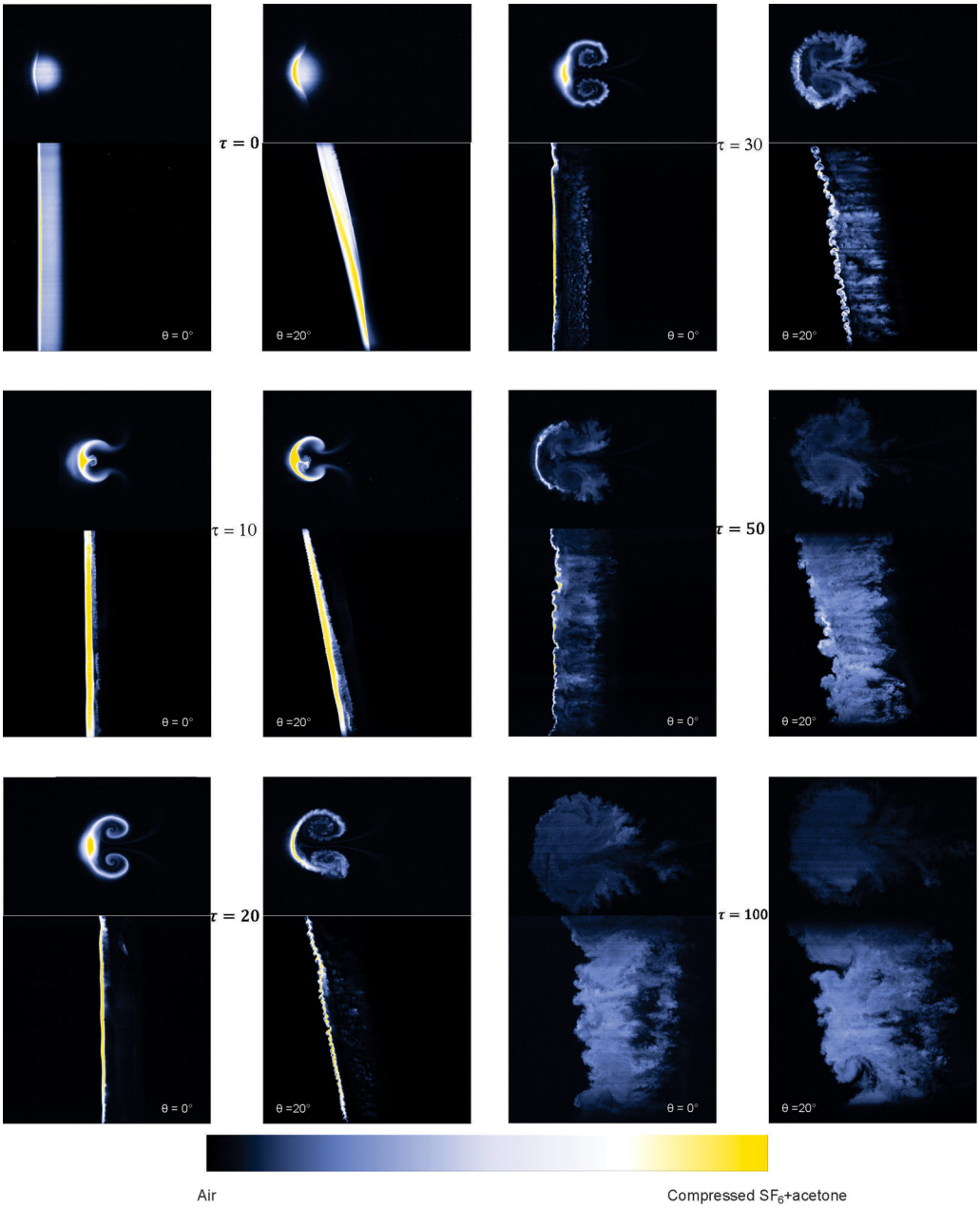

FIG. 2. Shock-accelerated gas cylinder evolution at $M = 2$ and $A = 0.6$ for tilt angles $\theta = 0$ and 20°. Images in the centerline (top) and vertical (bottom) planes are paired. Dimensionless time τ is labeled. The color is artificial and the streamwise image extent is 44 mm.

captured with a 4-megapixel backward-oriented and cooled CCD camera with 16 grayscale bits per pixel and a quantum efficiency of about 90%.

Figure 2 shows a comparison of flows evolving from quasi-two-dimensional initial conditions at $\theta = 0$ and from three-dimensional initial conditions at $\theta = 20°$. The dimensionless time used to label the images is $\tau = kA\Delta V(t - t_0)$, where k and ΔV are the wave number and the piston velocity

introduced earlier. For a cylinder of diameter D, $k = 2\pi/D$. Time $t = t_0$ corresponds to the shock traversing the center of the initial column. In terms of timing τ, the initial linear growth rates (1) would remain the same for the same geometry of the initial conditions, not changing with A or M (or, to be more exact, ΔV).

In both cases ($\theta = 0$ and $\theta = 20^\circ$), for a substantial amount of time, the flow in the centerline plane is dominated by a pair of counterrotating vortex columns well known from earlier studies. However, flow evolution in the vertical plane is different: For oblique shock interaction, vorticity of the same sign is deposited along the oblique density interfaces, leading to the formation of shear layerlike structures, emerging at $\tau = 10$ and clearly apparent at $\tau = 20$. Late-time images appear disordered, with multiple interacting vortices on multiple scales, and apparently increased mixing. Histogram analysis of the data sets [20] indeed strongly suggests that the flow shown in Fig. 2 undergoes a mixing transition [21] by time $\tau \sim 100$.

How can we quantify the apparent transition to turbulence here? Statistically, turbulence has long been associated with the power-law behavior of spectra within the inertial range. It is important to note that, while the spectral representation of Kolmogorov theory (the five-thirds law [22]) is perhaps better known, the original paper [17] actually dealt with real-space properties of turbulence based on two-point velocity correlations and the statistics of velocity structure functions based on real-space point-to-point distance r rather than wave number κ.

Velocity structure function evolution in a shock-accelerated heavy-gas cylinder flow was studied for small ($M = 1.2$) Mach numbers [14] with particle image velocimetry (PIV). The late-time results were roughly consistent with Kolmogorov's prediction of $2/3$ power-law scaling for the second-order longitudinal velocity structure function. Sadly, at higher Mach numbers, tracer particles used for PIV present an increasing problem because they do not follow the gas flow [23] and interfere with flow physics in nontrivial ways [18]. Here we use a cleaner diagnostic (PLIF); however, it does not easily yield results in terms of velocity, because it effectively shows cross sections of a scalar field (fluorescence intensity is related to tracer concentration and thus to local volume fraction of injected gas mixture) advected by the flow. In turbulent flow, such scalar fields are long known to develop power-law statistics as well. Corrsin [16] famously derived the equation for the spectrum of temperature fluctuations in isotropic fully developed turbulent flow with $k^{-5/3}$ exponent. This result can be generalized to the spectrum of any diffusive passive scalar and even of a reacting component in the flow [24] and moreover has an equivalent representation in terms of the second-order structure function of the scalar (under the same conditions that ensure the equivalence of the $-5/3$ and $2/3$ laws for velocity spectra and structure functions [24]). The second-order structure function of the scalar in fully developed turbulent flow should thus also scale as $r^{2/3}$. Power-law scaling emergence for a Mie scattering intensity field from submicron-sized particles premixed with a varicose curtain of heavy gas was reported [13] for a low-Mach-number (1.2) shock-driven flow over a range of more than one order of magnitude, with a 0.73 exponent. Again, it is important to caution that the addition of even a modest volume fraction of particles or droplets modifies the structure of turbulence, leading to changes in energy transfer rate and in flow anisotropy [25], so one must be careful in interpreting results of experiments with and without particle tracers: The flow statistics may not be the same.

Advances in image acquisition and experimental techniques now make it possible to resolve the entire range of physically relevant scales in laboratory shock-driven flow, from the energy injection scale (centimeter-sized baroclinically produced vortices) down to the Kolmogorov length scale (order of microns). With fluorescent gas as the tracer, flow tracking fidelity also ceases to be a problem at higher Mach numbers. Figure 3 shows plots of the second-order structure function $I_2(r)$ of fluorescence intensity I of the tracer after $M = 2$ shock acceleration, which should map the local concentration of the injected gas cylinder material (SF_6 with acetone): $I_2(r) = \langle [I(\mathbf{x}) - I(\mathbf{x} + \mathbf{r})]^2 \rangle$. Here $\langle \cdot \rangle$ denotes ensemble averaging over all pairs of points in the image separated by a distance $r = |\mathbf{r}|$. On the time scale of the experiments, differential diffusion of acetone and SF_6 plays no role.

Significant differences are apparent in the flow morphology at $\theta = 0$ and $\theta = 20^\circ$, especially in the vertical plane. These differences and the presence of notable anisotropy notwithstanding, the late-time ($\tau \sim 100$) behaviors of $I_2(r)$ are remarkably similar and close to a power law. What is also

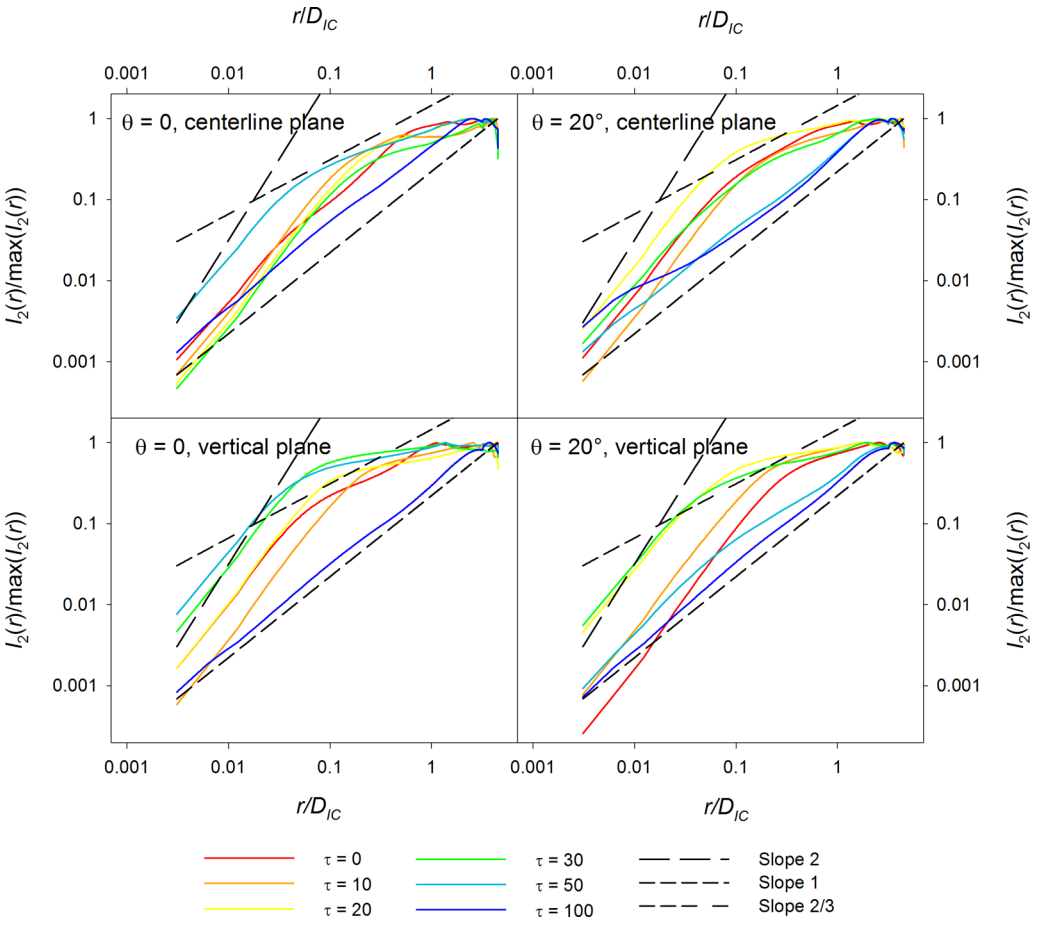

FIG. 3. Second-order structure functions of fluorescence intensity $I_2(r)$ in images shown in Fig. 2. The values of the structure functions are normalized by their maxima and r is scaled by the injection nozzle diameter D_{IC}. The plots are color coded by dimensionless times τ. Power-law scalings with exponents 2, 1, and 2/3 are shown as guides for the eye.

noteworthy is that the exponent of the best power-law fit to late-time $I_2(r)$ is appreciably higher than the fully developed turbulence prediction (2/3); in fact, it is close to unity. Moreover, this late-time behavior is quite prominent in the parameter space we investigated: $M = 1.13$, 1.4, 1.7, and 2.0 and $\theta = 0$, 20°, and 30°, manifesting over at least a decade in 17 out of 24 plots in Fig. 4.

In the context of the transition to turbulence, the formation of a cascade with power-law scaling of the structure functions is expected. In a sense, similar behavior across a range of different initial geometries and Mach numbers is also consistent with the notion of a transition to turbulence, when the flow "forgets" its initial conditions. A question that arises, however, is why $I_2(r)$ scales as r^1 rather than as $r^{2/3}$. Some of the likely answers are that the scaling emerges in flow that does not fit the definition of fully developed turbulence; it is transitional, driven by a finite energy input, and significantly anisotropic even at late times. Scalar spectra are well known to deviate from the Obukhov-Corrsin value [26] and this applies even to flows where the velocity field scaling is consistent with Kolmogorov theory predictions [27,28]. The latter reference is of specific interest because it deals with the transformation of a blob of scalar initially injected in the flow, which is not very far from our visualization scheme.

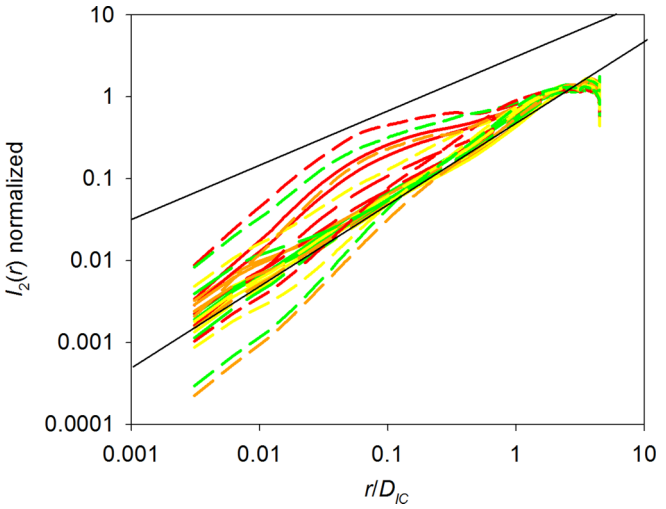

FIG. 4. Late-time ($\tau \gtrsim 100$) structure functions of fluorescence intensity $I_2(r)$ normalized by their average values for each image. Mach numbers are color coded: red, 1.1; orange, 1.4; yellow, 1.7; and green, 2.0. Solid lines denote $\theta = 0$, long-dashed lines $\theta = 20^\circ$, and short-dashed lines $\theta = 30^\circ$. Thin black lines show slopes of 2/3 (top) and 1 (bottom).

Velocity-field isotropy is very important for the Obukhov-Corrsin scalar scaling to manifest [27], because in most estimates of scalar dissipation, the assumption of local isotropy is used. Accordingly, significant deviation of scalar scaling from the 2/3 value is notable for shear flows [26,27]. In the flow under consideration here, shear plays a major role both in the formation of secondary instabilities in the centerline plane and in the apparent Kelvin-Helmholtz vortex formation in the vertical plane. While the scalar structure function scaling we observe is not totally physically unexpected, it is quite interesting and deserves further study.

This work was supported by the US Department of Energy Grant No. DE-NA-0002913.

[1] R. D. Richtmyer, Taylor instability in shock acceleration of compressible fluids, Commun. Pure Appl. Math. **13**, 297 (1960).

[2] E. E. Meshkov, Instability of the interface of two gases accelerated by a shock wave, Izv. Akad. Nauk SSSR, Mekh. Zhidk. Gaza **4**, 151 (1969).

[3] A. Burrows, J. Hayes, and B. A. Fryxell, On the nature of core-collapse supernova explosions, Astrophys. J. **450**, 430 (1995).

[4] C. C. Wu and P. H. Roberts, Richtmyer-Meshkov instability and the dynamics of the magnetosphere, Geophys. Res. Lett. **26**, 655 (1999).

[5] V. N. Goncharov, Theory of the Ablative Richtmyer-Meshkov Instability, Phys. Rev. Lett. **82**, 2091 (1999).

[6] J. Yang, T. Kubota, and E. E. Zukoski, Applications of shock-induced mixing to supersonic combustion, AIAA J. **31**, 854 (1993).

[7] M. Brouillette, The Richtmyer-Meshkov instability, Annu. Rev. Fluid Mech. **34**, 445 (2002).

[8] P. Vorobieff and S. Kumar, Experimental studies of Richtmyer-Meshkov instability, Rec. Res. Dev. Fluid Dyn. **5**, 33 (2004).

[9] Y. Yang, Q. Zhang, and D. H. Sharp, Small amplitude theory of Richtmyer-Meshkov instability, Phys. Fluids **6**, 1856 (1994).

[10] Q. Zhang and S.-I. Sohn, Nonlinear theory of unstable fluid mixing driven by shock wave, Phys. Fluids **9**, 1106 (1997).

[11] O. Sadot, L. Erez, D. Oron, G. Erez, G. Ben-Dor, U. Alon, L. A. Levin, and D. Shvarts, Studies on the nonlinear evolution of the Richtmyer-Meshkov instability, Astrophys. J. Suppl. Ser. **127**, 469 (2000).

[12] P. M. Rightley, P. Vorobieff, R. Martin, and R. F. Benjamin, Experimental observations of the mixing transition in a shock-accelerated gas curtain, Phys. Fluids **11**, 186 (1999).

[13] P. Vorobieff, P. M. Rightley, and R. F. Benjamin, Power-Law Spectra of Incipient Gas-Curtain Turbulence, Phys. Rev. Lett. **81**, 2240 (1998).

[14] P. Vorobieff, N.-G. Mohamed, C. Tomkins, C. Goodenough, M. Marr-Lyon, and R. F. Benjamin, Scaling evolution in shock-induced transition to turbulence, Phys. Rev. E **68**, 065301 (2003).

[15] A. M. Obukhov, The structure of the temperature field in a turbulent flow, Izv. Akad. Nauk SSSR, Ser. Geogr. Geophys. **13**, 58 (1949).

[16] S. Corrsin, On the spectrum of isotropic temperature fluctuations in an isotropic turbulence, J. Appl. Phys. **22**, 469 (1951).

[17] A. N. Kolmogorov, The local structure of turbulence in incompressible viscous fluid for very large Reynolds numbers, Dokl. Akad. Nauk SSSR **30**, 299 (1941).

[18] P. Vorobieff, M. Anderson, J. Conroy, R. White, C. R. Truman, and S. Kumar, Vortex Formation in Shock-Accelerated Gas Induced by Particle Seeding, Phys. Rev. Lett. **106**, 184503 (2011).

[19] M. Anderson, Oblique shock interactions with perturbed density interfaces, Ph.D. thesis, University of New Mexico, 2012.

[20] D. Olmstead, P. Wayne, J.-H. Yoo, S. Kumar, C. R. Truman, and P. Vorobieff, Experimental study of shock-accelerated inclined heavy gas cylinder, Exp. Fluids **58**, 71 (2017).

[21] P. E. Dimotakis, The mixing transition in turbulent flows, J. Fluid Mech. **409**, 69 (2000).

[22] A. N. Kolmogorov, A refinement of previous hypotheses concerning the local structure of turbulence in a viscous incompressible fluid at high Reynolds number, J. Fluid Mech. **13**, 82 (1962).

[23] M. Anderson, P. Vorobieff, C. R. Truman, C. Corbin, G. Kuehner, P. Wayne, J. Conroy, R. White, and S. Kumar, An experimental and numerical study of shock interaction with a gas column seeded with droplets, Shock Waves **25**, 107 (2015).

[24] A. S. Monin and A. M. Yaglom, in *Statistical Fluid Mechanics, Volume II: Mechanics of Turbulence*, edited by J. L. Lumley (Courier, Mineola, 2013).

[25] S. Elghobashi and G. C. Truesdell, On the two-way interaction between homogeneous turbulence and dispersed solid particles. I: Turbulence modification, Phys. Fluids A **5**, 1790 (1993).

[26] A. Celani, M. Cencini, M. Vergassola, E. Villermaux, and D. Vincenzi, Shear effects on passive scalar spectra, J. Fluid Mech. **523**, 99 (2005).

[27] K. R. Sreenivasan, The passive scalar spectrum and the Obukhov-Corrsin constant, Phys. Fluids **8**, 189 (1996).

[28] E. Villermaux, C. Innocenti, and J. Duplat, Short circuits in the Corrsin-Obukhov cascade, Phys. Fluids **13**, 284 (2001).